



HAL
open science

GLRX5 mutations impair heme biosynthetic enzymes ALA synthase 2 and ferrochelatase in Human congenital sideroblastic anemia

Raed Daher, Abdellah Mansouri, Alain Martelli, Sophie Bayart, Hana Manceau, Isabelle Callebaut, Boualem Moulouel, Laurent Gouya, Hervé Puy, Caroline Kannengiesser, et al.

► To cite this version:

Raed Daher, Abdellah Mansouri, Alain Martelli, Sophie Bayart, Hana Manceau, et al.. GLRX5 mutations impair heme biosynthetic enzymes ALA synthase 2 and ferrochelatase in Human congenital sideroblastic anemia. *Molecular Genetics and Metabolism*, 2019, 10.1016/j.ymgme.2018.12.012 . hal-02351427

HAL Id: hal-02351427

<https://hal.science/hal-02351427v1>

Submitted on 21 Jul 2022

HAL is a multi-disciplinary open access archive for the deposit and dissemination of scientific research documents, whether they are published or not. The documents may come from teaching and research institutions in France or abroad, or from public or private research centers.

L'archive ouverte pluridisciplinaire **HAL**, est destinée au dépôt et à la diffusion de documents scientifiques de niveau recherche, publiés ou non, émanant des établissements d'enseignement et de recherche français ou étrangers, des laboratoires publics ou privés.



Distributed under a Creative Commons Attribution - NonCommercial 4.0 International License

***GLRX5* mutations impair heme biosynthetic enzymes ALA synthase 2 and ferrochelatase in Human congenital sideroblastic anemia**

Short title: Mutated *GLRX5* in congenital sideroblastic anemia

Authors: Raêd Daher^{1-3,7,9}, Abdellah Mansouri^{1,2}, Alain Martelli⁴, Sophie Bayart⁵, Hana Manceau¹⁻³, Isabelle Callebaut⁶, Boualem Moulouel⁷, Laurent Gouya^{1-3,7}, Hervé Puy^{1-3,7*}, Caroline Kannengiesser^{1-3,9*} and Zoubida Karim^{1-3*}.

Affiliations :

¹INSERM U1149, Centre de Recherche sur l'inflammation (CRI), Paris, France.

²Université Paris Diderot, site Bichat, Sorbonne Paris cité, Paris, France, DHU UNITY

³Laboratory of excellence GR-Ex, Paris, France.

⁴Department of Translational Medicine and Neurogenetics, Illkirch, France, currently at Rare Disease Research Unit, Pfizer Inc., Cambridge, MA, USA.

⁵Department of Pediatric Hematology, Hôpital Sud, CHU Rennes, France.

⁶CNRS UMR7590, Sorbonne Universités, Université Pierre et Marie Curie-Paris6-MNHN-IRD-IUC, Paris, France.

⁷AP-HP, Centre Français des Porphyries (CFP), Hôpital Louis Mourier, Colombes, France.

⁸Hematology Laboratory CHU de Rennes, Pôle Biologie, Rennes, France.

⁹AP-HP, Département de Génétique, Hôpital Bichat, Paris, France.

¹⁰CHU Rennes, Liver disease and Molecular Genetics department, Rennes, France.

***C.K., H.P. and Z.K. contributed equally to this work**

Corresponding author: Herve Puy, MD, PhD

INSERM U1149. Université Paris Diderot, site Bichât, 16 rue Henri Huchard,
75018 Paris, France. E-mail: herve.puy@aphp.fr

Abstract

Non-syndromic microcytic congenital sideroblastic anemia (cSA) is predominantly caused by defective genes encoding for either ALAS2, the first enzyme of heme biosynthesis pathway or SLC25A38, the mitochondrial importer of glycine, an ALAS2 substrate. Herein we explored a new case of cSA with two mutations in *GLRX5*, a gene for which only two patients have been reported so far. The patient was a young female with biallelic compound heterozygous mutations in *GLRX5* (p.Cys67Tyr and p.Met128Lys). Three-D structure analysis confirmed the involvement of Cys67 in the coordination of the [2Fe-2S] cluster and suggested a potential role of Met128 in partner interactions. The protein-level of ferrochelatase, the terminal-enzyme of heme process, was increased both in patient-derived lymphoblastoid and CD34+ cells, however, its activity was drastically decreased. The activity of ALAS2 was found altered and possibly related to a defect in the biogenesis of its co-substrate, the succinyl-CoA. Thus, the patient exhibits both a very low ferrochelatase activity without any accumulation of porphyrins precursors in contrast to what is reported in erythropoietic protoporphyria with solely impaired ferrochelatase activity. A significant oxidative stress was evidenced by decreased reduced glutathione and aconitase activity, and increased MnSOD protein expression. This oxidative stress depleted and damaged mtDNA, decreased complex I and IV activities and depleted ATP content. Collectively, our study demonstrates the key role of *GLRX5* in modulating ALAS2 and ferrochelatase activities and in maintaining mitochondrial function.

Key words: GLRX5, sideroblastic anemia, porphyrins, mitochondria, heme, iron

Abbreviations

α -ketoglutarate dehydrogenase (KGDH)

α -lipoic acid (LA)

5- Delta-Aminolevulinic acid (ALA)

Aconitase (ACO)

Bovine serum albumin (BSA)

Congenital SA (cSA)

Cytochrome c oxidase, subunit 2 (COX 2)

Delta-aminolevulinic acid synthase 1 (ALAS1)

Delta-aminolevulinic acid synthase 2 (ALAS2)

Erythropoietic protoporphyria (EPP)

Erythropoietin (EPO)

Ferrochelatase (FECH)

Glutaredoxin-5 (*GLRX5*)

Glycophorin A (GPA)

Iron concentration in the liver (LIC)

Lymphoblastoid cell lines (LCLs)

Manganese superoxide dismutase (MnSOD)

Protoporphyrin IX (PPIX)

Pyruvate dehydrogenase (PDH)

Reduced form of glutathione (GSH)

Sideroblastic anemias (SA)

Transferrin receptor 1 (TfR1)

Acknowledgements

We are very grateful to the patient and her family who kindly contributed to this study. We also thank Aurélie Eisenmann (IGBMC, Illkirch) and Sylvie Simonin (CFP, Colombes) for their technical help, and Marianne Pons and Marielle ROMET (Santé Active Edition) for their assistance in medical writing.

Funding

INSERM and Paris Diderot University, France supported this work. Raed Daher was supported by the Laboratory of excellence GR-Ex, Paris, France, reference ANR-11-LABX-0051, which is funded by the program “Investissements d’avenir ” of the French National Research Agency, reference ANR-11-IDEX-0005-02. We are very grateful to “Association LEYLA” for supporting Raed Daher’s congress participation.

No potential conflict of interest relevant to this article was reported.

1. Introduction

Sideroblastic anemias (SA) comprise a heterogeneous group of congenital and acquired hematological disorders characterized by ring sideroblasts in the bone marrow with mitochondrial iron accumulation and often decreased heme synthesis [1,2]. The majority of those deposits are in the form of perinuclear mitochondrial ferritin, a novel iron-storage protein encoded by an intronless gene located on chromosome 5q23.1 [3]. Acquired SA generally occurs in association with myelodysplastic syndromes, but also as a result of alcohol or drug abuse, and nutritional deficiency in pyridoxine.

Congenital SA (cSA) is rare and has been associated with several germline mutations. The most common form of non-syndromic cSAs is X-linked and results from mutation in *ALAS2* gene encoding delta-aminolevulinic acid synthase 2 (ALAS2), the initial enzyme in the heme biosynthetic pathway in erythroid precursors [4]. Most of the *ALAS2* mutations are missense and affect the affinity of the enzyme for its cofactor, pyridoxal phosphate. In such cases, affected patients respond efficiently to oral pyridoxine treatment. However, we have previously reported C-terminal deletions with gain-of-function in *ALAS2* in families with an erythropoietic protoporphyria (EPP) phenotype but no SA or iron overload [5]. This X-linked dominant protoporphyria is characterized by a markedly increased ALAS2 activity and significant accumulation of the last heme-precursor, protoporphyrin IX (PPIX) exceeding iron availability in erythrocytes [5]. Although, the ferrochelatase (FECH), the last enzyme in the heme biosynthetic pathway, is crucial for the incorporation of iron in PPIX to produce heme, congenital erythropoietic porphyria (EPP) that is associated with defect in

ferrochelatase activity and normal ALAS2 is rather associated with PPIX accumulation [6,7].

Variations in the gene for the glycine mitochondrial carrier *SLC25A38* have also been reported in patients with recessive cSA [8,9]. At last, two cases of recessive cSA caused by mutations in glutaredoxin-5 (*GLRX5*) have been described [10,11]. A homozygous mutation in *GLRX5* interfering with intron 1 splicing was identified in 2007 in a patient presenting a sideroblastic-like microcytic anemia and iron overload [10]. *GLRX5* is a 156-amino acid mitochondrial protein that belongs to the glutaredoxin (GRX) family. GRX are small proteins with a thiol reductase activity known to regulate the redox state of cysteine residues using the reduced form of glutathione (GSH) as electron donor [12]. Studies have also shown that *GLRX5* is required for the assembly of iron-sulfur Fe-S clusters [13–15]. Indeed, *GLRX5* is abundant in erythroid cells. It has been shown to homodimerize and assemble [2Fe-2S] at the N-terminal active site cysteine (Cys67) thiols consisting of two subunits and two cysteine thiols from two GSH [16,17]. Thus, *GLRX5* may play an essential role in heme biosynthesis since the activity of FECH enzyme itself is dependent to [2Fe-2S] clusters [18].

Mutations in *HSPA9*, a mitochondrial HSP70 homolog, are also responsible for causing cSA [19]. Described mutations are transmitted as an autosomal recessive trait, but a pseudodominant pattern of inheritance occasionally occurs due to a common *HSPA9* allele, resulting in lower *HSPA9* expression.

Besides these genetically defined non-syndromic forms of cSA, syndromic forms have also been described. They are recognized due to mutations in *ABCB7* encoding a mitochondrial Fe-S transporter [20], *PUS1* encoding a pseudouridine

synthase [21], *SLC19A2* encoding a thiamine transporter [22], *TRNT1* encoding a CCA-adding enzyme [23], *YARS2* encoding a mitochondrial protein that catalyzes the attachment of tyrosine to tRNA(Tyr) [24], *NDUFB11* encoding a complex I subunit [25], and finally deletions in mitochondrial DNA (Pearson syndrome) [26]. The 16.569 base pair closed circular molecule of human mitochondrial DNA (mtDNA) encodes 13 of the respiratory chain polypeptides, as well as the two ribosomal RNAs and 22 transfer RNAs required for their mitochondrial synthesis [27]. mtDNA is 10-16 times more prone to oxidative damage than nuclear DNA (nDNA), because of its lack of protective histones, its poor repair capacity, and its attachment to the mitochondrial inner membrane, the main source of oxygen radicals in the cell [28]. The iron-induced oxidative stress causes the formation of 8-hydroxydeoxyguanosine in mtDNA as well as apurinic/aprimidinic sites and mtDNA strand breaks. These mtDNA lesions can lead to mtDNA depletion in animals and to premature mtDNA deletions in humans [29]. Iron overload can therefore decrease the synthesis of the 13 mtDNA-encoded proteins including subunits of the respiratory chain complexes I, III, IV and V, leading to mitochondrial dysfunction.

Herein, in order to gain more insight into the role played by GLRX5 in the heme biosynthetic pathway, we explored a third case with compound heterozygous missense mutations in *GLRX5*: p.Cys67Tyr and p.Met128Lys. We also performed functional analyses to measure intracellular iron metabolism, heme biosynthesis, mitochondrial function and Fe-S clusters assembly.

2. Methods

2.1 Patient

The patient was subsequently referred to the Department of Genetics at Bichât Hospital (Paris, France) in 2014 for molecular exploration of genes implicated in SA. Written informed consent was obtained from the patient and her parents and from control subjects in accordance with the Declaration of Helsinki.

2.2 *GLRX5* sequencing

DNA was prepared from peripheral blood leukocytes using QIAamp DNA Blood Mini Kit (Qiagen, Courtaboeuf Cedex, France). *GLRX5* 2 exons and flanking sequences were amplified by PCR. The two strands of PCR products were sequenced using the BigDye Terminator Cycle Sequencing Ready Reaction kit on an ABI PRISM 3130xl sequencer (Applied Biosystems, Life Technologies, Courtaboeuf Cedex, France). *GLRX5* sequencing primers are shown in Supplemental Table S1. Sequencing data were examined with Seqscape v2.6.0 software.

2.3 Cell culture

Lymphoblastoid cell lines (LCLs) generated from the patient and 4 unrelated healthy subjects were cultured in RPMI 1640 medium (Gibco, Life Technologies, Courtaboeuf Cedex, France) supplemented with 10% fetal bovine serum, 2% L-Glutamine 200mM (100X) (Gibco, Life Technologies, Courtaboeuf Cedex, France), 1% HEPES 1 mM (Gibco, Life Technologies, Courtaboeuf Cedex, France), 1% penicillin-streptomycin solution, at 37°C and 5% CO₂ in the air.

To obtain CD34+ cells from the *GLRX5* patient and a counterpart healthy control, mononuclear cells were isolated from 60 ml peripheral whole blood, by Ficoll density-gradient centrifugation (LSM; PAA laboratories, Velizy Villacoublay,

France). CD34⁺ cells were then purified by positive selection using immunomagnetic beads (MACS CD34 MicroBead Kit; Miltenyi Biotec, Bergisch Gladbach, Germany) and lead to grow for 6 days in erythroid differentiation medium (Iscove modified Dulbecco medium) (Invitrogen, California, USA) supplemented with 3% human serum type AB (Sigma-Aldrich, Saint-Quentin-Fallavier, France), 2% human peripheral blood plasma (StemCell Technologies), 10 µg/mL human insulin (Sigma-Aldrich, Saint-Quentin-Fallavier, France), 3 UI/mL heparin (Sigma-Aldrich, Saint-Quentin-Fallavier, France), 3 UI/mL erythropoietin (EPO) (Janssen-Cilag, Issy-les-Moulineaux, France), 10 ng/mL SCF, 1 ng/mL IL-3 et 10 ng/mL interleukin 3 (IL-3) (Miltenyi Biotec, Bergisch Gladbach, Germany) and 200 µg/mL human holo-transferrin (Sigma-Aldrich, Saint-Quentin-Fallavier, France). From day 7 to day 10, IL-3 was omitted from the culture medium and the concentration of EPO was adjusted to 1 UI/mL. Cells were cultured at 37°C in an atmosphere of 5% CO₂ in the air. All experiments performed on both LCLs and CD34⁺ cultures were realized at least in triplicate.

2.4 Measurement of total ferritin level

Total ferritin level was measured in cell lysates using an AU400 automate (Beckman Coulter France S.A.S., Villepinte Roissy, France).

2.5 ALA induced accumulation of PPIX

5-Delta-aminolevulinic acid (ALA) was diluted in water and added to the cell culture medium at a final concentration of 300 µM and incubated for 24 h, at day 9 of erythroid differentiation. On million cells were washed twice with PBS 0.5% BSA buffer and cellular content of PPIX was measured by flow cytometry (Ex. 605, Em. 655 nm).

2.6 Flow cytometry

Cells were analyzed for surface expression of glycoprotein A (GPA), CD36, and CD71. One million cells were washed in PBS supplemented with 0.5% bovine serum albumin (BSA) and stained with fluorochrome-conjugated antibodies for 20 minutes on ice. IgG-FITC (Beckman Coulter, Marseille, France) was used as negative control. Cells were washed once with PBS 0.5% BSA before analysis. The samples were analyzed by using BD LSRFortessa flow cytometer and FlowJo software (BD Biosciences, Rungis, France).

2.7 Measurement of ATP level

Fresh cell pellets were ground in liquid nitrogen and transferred into 500 μ L of ice-cold 1 M perchloric acid. After centrifugation at 4°C, aliquots were neutralized with 5 M K_2CO_3 and centrifuged at 4°C. The pellet was used to determine protein content, and the supernatant was used to measure ATP with a luciferin-luciferase assay kit following the manufacturer's recommendations (Roche Diagnostics, Mannheim, Germany).

2.8 Measurement of aconitase and citrate synthase activities

To assess aconitase activity, total fresh cells and mitochondrial or cytosolic fractions were homogenized in 100 μ L of buffer (50 mM Tris HCl, pH 7.4, 0.2 mM sodium citrate, and 0.05 mM $MgCl_2$). Homogenates were centrifuged at 800 g at 4°C for 10 min, and supernatants were sonicated for 20 seconds. Proteins (100 μ g) were incubated at 37°C for 5 min with 1 mM sodium citrate, 1 mM NADP⁺ and 2 U isocitrate dehydrogenase. The formation of NADPH was measured from its absorption at 340 nm.

Citrate synthase activity was determined on the basis of the chemical coupling of CoA-SH released from Acetyl-CoA during citrate to 5,5-dithio-bis-(2-nitrobenzoic) acid synthesis. Activity was expressed as nmol of 5,5-dithio-bis-(2-nitrobenzoic) acid oxidized per minute and per milligram of protein.

2.9 Mitochondrial complex I and IV and citrate synthase activities

Submitochondrial particles were prepared by two cycles of freezing/thawing. Complex I (NAD ubiquinone oxidoreductase) was assayed by following the oxidation of NADH in the presence of decylubiquinone and antimycin A as described elsewhere [30].

2.10 Determination of GSH level

Reduced glutathione (GSH) levels were determined following a method adapted from Griffith [31].

2.11 Mitochondrial DNA level and structure.

Slot blot hybridization was used to look for mtDNA depletion [32]. mtDNA and nDNA were assessed by densitometry analysis of autoradiographs.

To detect mtDNA lesions, a long (5942-bp) and a short (464-bp) mtDNA fragments were amplified using the Expand Long PCR system (Roche Applied Science, Meylan Cedex, France) according to the manufacturer's instructions and 40 pmol of primers described in **supplemental Table S1**. To search for mtDNA strand breaks, proportions of mtDNA in its supercoiled, circular, and 16.5-kb linear forms were studied by Southern blot. Total DNA (5 µg) was loaded on 0.7% agarose gels without ethidium bromide, and electrophoresed overnight at 2.5 V/cm, transferred to a Hybond-N1 nylon membrane, and hybridized with the

5.942-kb human mtDNA probe. The mtDNA forms were quantified by densitometry of autoradiographs.

2.12 Statistical analysis

A two-tailed Student's t-test was used with a level of significance at $p < 0.05$. GraphPad InStat software (GraphPad Software, San Diego, CA) was used for statistical evaluation.

Additional methods are described in "Supplemental data".

3 Results

3.1 Patient characteristics

The patient, a 14-year old girl, presented with aregenerative microcytic anemia (MCV=60fL and Hb=8.9g/dL), iron overload and elevated serum ferritin level (466 µg/L) at the department of pediatric hematology, university hospital of Rennes (France) in 2012. Patient's biological characteristics are compiled in **Table 1**. For diagnosis of SA, a blind analysis of bone marrow and blood smears was performed by two independent experts (**Supplemental Figure S1**). Blood examination revealed severe anisopoikilocytosis, marked hypochromia, numerous elliptocytes, dacryocytes and fragmented red blood cells. Furthermore, few spherocytes were observed. Macrocytosis, defective hemoglobinization, binucleation, and dysgranulopoiesis with 12% type 1, 15% type 2 and 37% type 3 sideroblasts were found in the bone marrow. There was no apparent sign of dehydration and maximum deformability was decreased (data not shown). Iron concentration in the liver (LIC) and heart were assessed using two MRI protocols, signal intensity ratio and gradient echo imaging (R2*), which confirmed hepatic iron overload (LIC at 200 µmol/g) and no cardiac overload. Serum hepcidin measured by ELISA was undetectable. Patient did not have any hemolysis as shown by bilirubin (4.34 µmol/L) and LDH (385 UI/L) values within normal range. The patient started iron chelation therapy (Exjade, 15mg/kg) in November 2012. At the 6-month follow-up visit (in March 2013), the patient presented with flu and a hematologic panel performed 15 days later showed that anemia had worsened with hemoglobin (Hb) at 6.4 g/dL, which required a blood transfusion (Table 1). She was also prescribed Speciafoldine (5mg/day) and the ferritin level reached

191 µg/L. Her condition required a second transfusion in May 2013. Upon physical examination at the 1-year follow-up, paleness of skin and mucous membranes were visibly reduced and the patient was only complaining about fatigue. Blood tests showed an improvement with Hb at 9 g/dL and ferritin at 71 µg/L with no hepatic cytolysis as shown by aspartate aminotransferase (ASAT) at 80 IU/L and alanine aminotransferase (ALAT) at 167 IU/L.

3.2 Identification of *GLRX5* mutations

Sequencing of *GLRX5* (Ref Seq NM_016417; NP_057501) led to the identification of two heterozygous missense mutations: transition G>A at position 200 in exon 1 and T>A at position 383 in exon 2 causing the p.Cys67Tyr and p.Met128Lys amino acids substitutions, respectively (**Figure 1A**). Molecular exploration of patient's both parents showed that the mutation p.Cyst67Tyr was inherited from the father, while p.Met128Lys was inherited from the mother. Genetic analysis for eventual other involved genes was performed with next generation sequencing using a panel of 61 genes related to iron and heme metabolisms (**Supplemental data**) using patient's genomic DNA. The results did not reveal any mutation.

3.3 Impact of p.Cys67Tyr and p.Met128Lys *GLRX5* mutations on the 3D structure and *GLRX5* mRNA expression

Both p.Cys67Tyr and p.Met128Lys mutations affected highly conserved *GLRX5* amino acids throughout species (**Figure 1 B**). Analysis of the published crystal structure of human *GLRX5* [17] confirmed that the cysteine at position 67 is

directly involved in the coordination of the [2Fe-2S] clusters by GLRX5 (**Figure 1 C**). Of note, this cysteine substitution may also affect the stability of helix alpha-4, which is involved in glutathione (GSH) binding, and thus indirectly on iron-sulfur coordination. In contrast, methionine at position 128 is not located in the vicinity of the [2Fe-2S] cluster, but is exposed to the surface within a groove, suggesting that it might have a role in the interaction of GLRX5 with other partner proteins. Substitution of this methionine might thus impair this interaction.

GLRX5 mRNA expression quantified by RT-qPCR was not modified in the patient's LCL and CD34+ cells compared with controls (data not shown), indicating that the identified mutations do not impair *GLRX5* transcriptional process.

3.4 Impact of the *GLRX5* mutations on heme biosynthesis key enzymes expression and activity

Since GLRX5 is required for the assembly of Fe-S clusters and FECH activity is dependent on [2Fe-2S], we decided to first investigate the impact of *GLRX5* mutations on heme biosynthesis using erythroid CD34+ and LCL cells derived from the patient. In both cell types, *FECH* mRNA levels were similar to controls (**Figure 2A and supplemental Figure S2 A**), while protein expression was increased ($p < 0.05$) (**Figure 2C and Supplemental Figure S2 B**). An alteration of GLRX5 has been associated with a decrease in the expression level of FECH protein [11]. Since we did not observe this decrease in our patient, we analyzed the activity of FECH. For that purpose, we used LCL cells rather than CD34+ because the presence of a large amount of heme and hemoglobin in these erythroid cells interfered considerably with the FECH activity assay (data not

shown). The results in Table 2 showed that despite increased protein expression, FECH activity was significantly reduced in the patient's LCL cells. However, impairment of FECH activity is known to be associated with accumulation of porphyrins precursors as seen in EPP patients exhibiting deficient FECH and normal ALAS2 (Table 2). In our patient, this porphyric profile was different since total porphyrins and zinc protoporphyrin in the erythrocytes as well as total porphyrins in the plasma were all normal, indicating no accumulation (Table 2). To investigate whether ALAS2 was affected, which may explain this normal porphyric phenotype, we explored its expression level and activity in patient's CD34+ cells. The results showed no difference in the mRNA level but a slight increase in the protein expression of ALAS2, when compared to control (**Figure 2B and 2C**, respectively). We then quantified fluorescent PPIX accumulation in CD34+ cells at day 8 or day 10 of culture. The results in **Figure 2D** showed that compared to healthy control, the patient's CD34+ did not accumulate PPIX, in contrast to CD34+ derived from EPP patients, which exhibited significant accumulation of PPIX (**Figure 2E**). This strongly suggested an inhibition of ALAS2 activity in our cSA patient's cells.

ALA is the first compound in the porphyrin synthesis pathway, produced in erythroid cells by ALAS2, from glycine and succinyl-CoA. To test the hypothesis of an alteration of ALAS2 activity in our patient, we treated the CD34+ cells with ALA and then quantified the accumulation rate of PPIX in the cells of the patient and those of the healthy control. Although an intracellular PPIX accumulation was observed in both cultures, the level of this PPIX accumulation was significantly increased in the CD34+ cells of the patient compared to those of healthy

controls, confirming that the absence of PPIX accumulation in our patient is due to an ALAS2 activity defect (**Figure 2F**). Furthermore, we also found similar expression profile of ALAS1 in patient's LCL, suggesting common consequence failures related to *GLRX5* mutations (**Supplemental Figure S2 C**).

Succinyl-CoA is an essential substrate for ALAS1 and ALAS2 activities, and an impact on its content may directly affect the activity of these two enzymes. Succinyl-CoA production in the mitochondria results from the conversion of α -ketoglutarate catalyzed by α -ketoglutarate dehydrogenase (KGDH) in the citric acid cycle. KGDH activity depends on α -lipoic acid (LA) which biosynthesis requires a Fe-S cluster [33,34]. Hence, we next explored the LA content in KGDH protein by western blot using antibodies for α -lipoic acid-KGDH. Our results showed a decrease in LA-ratio in KGDH and in pyruvate dehydrogenase (PDH), another protein complex of the citric acid cycle and bearing also the LA cofactor (**Figure 3**). Thus, decreased level of LA levels might be driven by the *GLRX5* mutation and may be responsible for ALAS2 activity defect.

3.5 Mitochondrial function in cSA patient

Next, we investigated the mitochondrial function in the patient's LCL cells. We found that the activities of mitochondrial complexes I and IV were significantly reduced by 52.2% ($p < 0.001$) and 34% ($p < 0.05$), respectively, in the patient's LCL compared to controls, whereas they did not change in the EPP LCL cells (**Figure 4A**). As shown in **Figure 4B**, citrate synthase activity was normal in the cSA and the EPP LCL compared to controls cells, indicating that mitochondrial mass was similar in these groups. These data also suggested that only Fe-S dependent enzymatic activities were affected by the *GLRX5* mutations. In addition, ATP

levels were severely decreased in the cSA patient by 62.3% ($p < 0.001$) and to a lower extent by 37% ($p < 0.002$) in the EPP patient (**Figure 4C**).

Next, we analyzed the mtDNA and nDNA content in LCL cells. Our data showed a reduction in mtDNA but not in nDNA in the patient compared with controls (**Figure 4D lower panel**). In addition, we used long PCR to co-amplify a 5942-bp and a 464-bp mtDNA fragments (**Figure 4D, upper panel**). Random DNA lesions blocking replication are more likely to be present on a long DNA region than a short fragment. Indeed, the amplification of the 464-bp short DNA fragment was similar in the patient and the control (**Figure 4D, upper panel**). These results suggested that the mtDNA depletion in the patient might be due, in part, to the polymerase γ -blocking lesions on mtDNA templates, thus hampering mtDNA synthesis. The quality of mtDNA was also analyzed by southern blot hybridized with the mtDNA probe to analyze the supercoiled, circular, and linear (full-length) forms (**Figure 4E**). The results showed massive degradation of the patient's mtDNA compared to controls. Supercoiled mtDNA corresponds to unnicked mtDNA, circular mtDNA may correspond either to unnicked DNA or to mtDNA molecules with single strand nick(s), whereas the linear mtDNA is a form that has been cut on both strands. The topological organization of mtDNA was profoundly altered in the patient compared to controls. The intact supercoiled mtDNA form almost completely disappeared in favor of circular and linear mtDNA forms that consequently increased in the patient (**Figure 4E**). Finally, as shown by western blot analysis, mtDNA encoded cytochrome c oxidase, subunit 2 (COX 2) protein expression was markedly decreased in the patient (**Figure 4F, upper panel**) as a

result of reduced mtDNA levels. As expected, COX4 remained unchanged since it is encoded by nDNA (**Figure 4F, lower panel**).

3.6 Impact of *GLRX5* mutations on iron metabolism

To evaluate mitochondrial iron accumulation, total and cytosolic L-ferritin levels were measured in patient's LCL cells. Total ferritin was 2.7 fold increased in the total cell lysate (**Figure 5A**) with no change in the cytosolic fraction (**Figure 5B**), thereby confirming iron accumulation in the mitochondria and not in the cytosol. Determination of the amount of transferrin receptor 1 (TfR1) in the LCL cells by western blot (**Figure 5C, left panel**) and flow cytometry analysis (**Figure 5C, right panel**) did not reveal any difference between the patient and the control.

Next, we used western blot analysis to quantify the expression of the iron regulatory proteins IRP1 and IRP2 responsible for iron levels sensing. IRP2 protein expression was unchanged, while IRP1 level was significantly increased in the patient compared with control (protein level in **Figure 5D**, mRNA level in **Supplemental Figure S3**). In contrast to IRP2, IRP1 has a dual function and can act like an aconitase (ACO) in the presence of iron. Therefore, we measured the activity of cytosolic ACO1, i.e., IRP1, and that of mitochondrial ACO2. As shown in **Figure 5E**, only mitochondrial ACO2 activity was reduced, therefore, significantly decreasing the total aconitase activity by 78% ($p < 0.01$). These data suggested that IRP1 aconitase activity level was preserved in the patient's LCL cells, possibly as a result from a compensatory up-regulating mechanism at the translational level with an increase of the IRP1 protein.

3.7 Oxidative stress and cell proliferation in patient's LCL

The marked reduction by 56.8% ($p < 0.001$) in total GSH (**Figure 6A**) along with the increase in the mitochondrial antioxidant manganese superoxide dismutase (MnSOD) expression (**Figure 6B**), as well as oxidative damage to mtDNA (**Figures 4D and 4E**) in the patient's cells are direct indicators of oxidative stress in response to mitochondrial iron accumulation. Oxidative injury might explain why cells are not well proliferating as shown by the MTT cell viability assay (**Figure 6C**).

4 Discussion

In this study, we have documented a third case of cSA associated with two biallelic mutations in *GLRX5*: p.Cys67Tyr and p.Met128Lys. We found that these mutations affected functionally two important amino acid positions: one is involved in the [2Fe-2S] cluster coordination (Cys67) and the other potentially corresponds to an interaction site of GLRX5 with other partner proteins (Met128). Compared to the two previously reported cases who were 29 [10] and 44 [11] years old, our patient was only 14 years old. We can therefore postulate that the severity of cSA is not age-dependent. Her young age and the early initiation of an iron chelation therapy may also explain the absence of diabetes mellitus and dark skin at the time of diagnosis. In addition, our patient is female while the two other aforementioned subjects were males, demonstrating the presence of the disease in both genders.

The mutations in *GLRX5* reported in LCL cells from our patient are characterized by a defective Fe-S cluster assembly as suggested by diminished ferrochelatase and mitochondrial aconitase activities along with decreased complexes I and IV in the electron transport chain in which Fe-S clusters play an essential role. These findings are in agreement with previous studies [11,16,35]. However, we found that ACO1 activity remained intact in our patient. This suggests that Cys67 residue in GLRX5 which is implicated in [2Fe-2S] cluster biogenesis, may only affect ACO2 activity since ACO1 requires a [4Fe-4S] for its enzymatic activity. In a study published in 2010, Ye and colleagues reconstituted [2Fe-2S] bridged complexes into the purified human GLRX5 protein in an anaerobic chamber [16]. Using this approach, they have shown that the ligation

of [2Fe-2S] clusters between two monomers requires the catalytic residue Cys67 and external GSH. By performing site-directed mutagenesis, they found that Lys59, Thr108, and Asp123 residues were key players in the docking of the GSH ligand to GLRX5 protein. On the basis of these findings, they proposed that GLRX5 could function as a potential scaffold, delivering the preassembled [2Fe-2S] cluster to target proteins as previously suggested [36]. Biogenesis of cytosolic [4Fe-4S] may therefore not be impaired in our patient. This observation raises the possibility that IRP1 could be maintained in its cytosolic aconitase holoform with [4Fe-4S] clusters rather than its RNA-binding apo-form. As a consequence, there was no change in cytosolic iron levels as demonstrated by normal IRP2, TfR1 and cytosolic ferritin protein expression in our patient. Western blot analysis also revealed increased IRP1 protein expression. Although the underlying pathophysiological mechanisms are unknown, the decrease in heme biosynthesis might be responsible for a derepression of IRP1 translation as exogenous heme has been shown to negatively regulate IRP1 [37]. Reduced heme biosynthesis in the context of SA in our patient might also explain increased ALAS1 proteins expression in LCL cells. ALAS1 transcription is known to be negatively regulated by the heme [38]. However, assuming that the activities of ALAS1 and ALAS2 are both reduced in the context of *GLRX5* mutations, increased protein levels of both enzymes may be compensatory. Moreover, we have observed a dramatic reduction in ferrochelatase activity in our patient even more pronounced than in LCL cells from EPP patients. However, in contrast with EPP, total porphyrins and PPIX did not accumulate either in LCL cells, erythrocytes or plasma from the patient carrying the *GLRX5* mutations.

Interestingly this is the first report in Human of a drastic reduction of FeCh activity without any PPIX overload. These observations are in favor of a marked reduction in the activity of ALAS2, the enzyme that catalyzes the initial step in the heme biosynthetic pathway. This decrease could result from diminished LA synthesis. Newly identified biallelic mutations in *GLRX5* were recently described as a novel causal mechanism for decreased mitochondrial lipoylation in patients with a biochemical phenotype of non-ketotic hyperglycinemia [39]. These data indicated that *GLRX5* is likely a key player in the pathway that provides a Fe-S cluster to the lipoate synthase [39]. In another *in vitro* study, missense mutations introduced to the human *GLRX5* protein interfered with lipoate biosynthesis in K562 cells [35]. Taken together, these observations may support that the reduced LA content reported in our patient could be driven by the mutated *GLRX5*.

Our results also revealed that *GLRX5* mutations were associated with iron accumulation in mitochondria of LCL cells derived from the patient, together with abnormalities in the mtDNA profile and reduced levels of functional supercoiled mtDNA and oxidative stress illustrated by an increase in MnSOD expression and a decrease in GSH pool. This confirms the results of previous studies showing that iron excess (but also iron deficiency) was linked to mitochondrial dysfunction and mtDNA damage along with oxidative stress [40]. In our study, mitochondrial dysfunction was characterized by a significant reduction of complexes I and IV activities and severely decreased ATP level.

5 Conclusion

In the case reported here, biallelic compound heterozygous mutations p.Cys67Tyr and p.Met128Lys in *GLRX5* are responsible for the cSA phenotype in a young female patient. The mutated GLRX5 affected both ALAS and ferrochelatase activities, mitochondrial function and cell viability. In addition to its involvement in Fe-S clusters biosynthesis, GLRX5 seems to be important in succinyl-CoA biogenesis. Overall, defective GLRX5 leads to the alteration of heme biosynthesis without accumulation of porphyrin precursors, in contrast with porphyria disease.

Authorship contributions

Contribution: study concept and design: C.K., Z.K., H.P.; acquisition of patient data: S.B., L.S., AM.J.; patients' DNA sequencing: C.O., Analysis and interpretation of patient data: H.P., C.K., K.P.; conducting experiments or material support: R.D., A.M., A.M., T.L., N.D.; 3D structure analysis study: I.C.; Study supervision: Z.K.; critical revision of the manuscript for important intellectual content: Z.K., H.P., C.K.; Drafting of the manuscript: R.D., Z.K.; All authors participated in data discussion, read and approved the manuscript.

The Paper Explained:

- *GLRX5* mutations in a case of congenital sideroblastic anemia
- *GLRX5* role in maintaining mitochondrial function and heme biosynthesis.

References

- [1] A.K. Bergmann, D.R. Campagna, E.M. McLoughlin, S. Agarwal, M.D. Fleming, S.S. Bottomley, E.J. Neufeld, Systematic molecular genetic analysis of congenital sideroblastic anemia: evidence for genetic heterogeneity and identification of novel mutations, *Pediatr. Blood Cancer*. 54 (2010) 273–278. doi:10.1002/pbc.22244.
- [2] M. Cazzola, L. Malcovati, Diagnosis and treatment of sideroblastic anemias: from defective heme synthesis to abnormal RNA splicing, *Hematol. Am. Soc. Hematol. Educ. Program*. 2015 (2015) 19–25. doi:10.1182/asheducation-2015.1.19.
- [3] M. Cazzola, R. Invernizzi, G. Bergamaschi, S. Levi, B. Corsi, E. Travaglini, V. Rolandi, G. Biasiotto, J. Drysdale, P. Arosio, Mitochondrial ferritin expression in erythroid cells from patients with sideroblastic anemia, *Blood*. 101 (2003) 1996–2000. doi:10.1182/blood-2002-07-2006.
- [4] C. Camaschella, Recent advances in the understanding of inherited sideroblastic anaemia, *Br. J. Haematol*. 143 (2008) 27–38. doi:10.1111/j.1365-2141.2008.07290.x.
- [5] S.D. Whatley, S. Ducamp, L. Gouya, B. Grandchamp, C. Beaumont, M.N. Badminton, G.H. Elder, S.A. Holme, A.V. Anstey, M. Parker, A.V. Corrigall, P.N. Meissner, R.J. Hift, J.T. Marsden, Y. Ma, G. Mieli-Vergani, J.-C. Deybach, H. Puy, C-terminal deletions in the ALAS2 gene lead to gain of function and cause X-linked dominant protoporphyria without anemia or iron overload, *Am. J. Hum. Genet*. 83 (2008) 408–414. doi:10.1016/j.ajhg.2008.08.003.
- [6] H. Puy, L. Gouya, J.-C. Deybach, Porphyrias, *Lancet Lond. Engl*. 375 (2010) 924–937. doi:10.1016/S0140-6736(09)61925-5.
- [7] Z. Karim, S. Lyoumi, G. Nicolas, J.-C. Deybach, L. Gouya, H. Puy, Porphyrias: A 2015 update, *Clin. Res. Hepatol. Gastroenterol*. 39 (2015) 412–425. doi:10.1016/j.clinre.2015.05.009.
- [8] C. Kannengiesser, M. Sanchez, M. Sweeney, G. Hetet, B. Kerr, E. Moran, J.L. Fuster Soler, K. Maloum, T. Matthes, C. Oudot, A. Lascaux, C. Pondarré, J. Sevilla Navarro, S. Vidyatilake, C. Beaumont, B. Grandchamp, A. May, Missense SLC25A38 variations play an important role in autosomal recessive inherited sideroblastic anemia, *Haematologica*. 96 (2011) 808–813. doi:10.3324/haematol.2010.039164.
- [9] D.L. Guernsey, H. Jiang, D.R. Campagna, S.C. Evans, M. Ferguson, M.D. Kellogg, M. Lachance, M. Matsuoka, M. Nightingale, A. Rideout, L. Saint-Amant, P.J. Schmidt, A. Orr, S.S. Bottomley, M.D. Fleming, M. Ludman, S. Dyack, C.V. Fernandez, M.E. Samuels, Mutations in mitochondrial carrier family gene SLC25A38 cause nonsyndromic autosomal recessive congenital sideroblastic anemia, *Nat. Genet*. 41 (2009) 651–653. doi:10.1038/ng.359.
- [10] C. Camaschella, A. Campanella, L. De Falco, L. Boschetto, R. Merlini, L. Silvestri, S. Levi, A. Iolascon, The human counterpart of zebrafish shiraz shows sideroblastic-like microcytic anemia and iron overload, *Blood*. 110 (2007) 1353–1358. doi:10.1182/blood-2007-02-072520.

- [11] G. Liu, S. Guo, G.J. Anderson, C. Camaschella, B. Han, G. Nie, Heterozygous missense mutations in the GLRX5 gene cause sideroblastic anemia in a Chinese patient, *Blood*. 124 (2014) 2750–2751. doi:10.1182/blood-2014-08-598508.
- [12] A. Holmgren, Thioredoxin and glutaredoxin systems, *J. Biol. Chem.* 264 (1989) 13963–13966.
- [13] M.T. Rodríguez-Manzanegue, J. Tamarit, G. Bellí, J. Ros, E. Herrero, Grx5 is a mitochondrial glutaredoxin required for the activity of iron/sulfur enzymes, *Mol. Biol. Cell.* 13 (2002) 1109–1121. doi:10.1091/mbc.01-10-0517.
- [14] U. Mühlenhoff, J. Gerber, N. Richhardt, R. Lill, Components involved in assembly and dislocation of iron-sulfur clusters on the scaffold protein Isu1p, *EMBO J.* 22 (2003) 4815–4825. doi:10.1093/emboj/cdg446.
- [15] F. Vilella, R. Alves, M.T. Rodríguez-Manzanegue, G. Bellí, S. Swaminathan, P. Sunnerhagen, E. Herrero, Evolution and cellular function of monothiol glutaredoxins: involvement in iron-sulphur cluster assembly, *Comp. Funct. Genomics.* 5 (2004) 328–341. doi:10.1002/cfg.406.
- [16] H. Ye, S.Y. Jeong, M.C. Ghosh, G. Kovtunovych, L. Silvestri, D. Ortillo, N. Uchida, J. Tisdale, C. Camaschella, T.A. Rouault, Glutaredoxin 5 deficiency causes sideroblastic anemia by specifically impairing heme biosynthesis and depleting cytosolic iron in human erythroblasts, *J. Clin. Invest.* 120 (2010) 1749–1761. doi:10.1172/JCI40372.
- [17] C. Johansson, A.K. Roos, S.J. Montano, R. Sengupta, P. Filippakopoulos, K. Guo, F. von Delft, A. Holmgren, U. Oppermann, K.L. Kavanagh, The crystal structure of human GLRX5: iron-sulfur cluster co-ordination, tetrameric assembly and monomer activity, *Biochem. J.* 433 (2011) 303–311. doi:10.1042/BJ20101286.
- [18] R.A. Wingert, J.L. Galloway, B. Barut, H. Foott, P. Fraenkel, J.L. Axe, G.J. Weber, K. Dooley, A.J. Davidson, B. Schmid, B. Schmidt, B.H. Paw, G.C. Shaw, P. Kingsley, J. Palis, H. Schubert, O. Chen, J. Kaplan, L.I. Zon, Tübingen 2000 Screen Consortium, Deficiency of glutaredoxin 5 reveals Fe-S clusters are required for vertebrate haem synthesis, *Nature*. 436 (2005) 1035–1039. doi:10.1038/nature03887.
- [19] K. Schmitz-Abe, S.J. Ciesielski, P.J. Schmidt, D.R. Campagna, F. Rahimov, B.A. Schilke, M. Cuijpers, K. Rieneck, B. Lausen, M.L. Linenberger, A.K. Sendamarai, C. Guo, I. Hofmann, P.E. Newburger, D. Matthews, A. Shimamura, P.J.L.M. Snijders, M.C. Towne, C.M. Niemeyer, H.G. Watson, M.H. Dziegiel, M.M. Heeney, A. May, S.S. Bottomley, D.W. Swinkels, K. Markianos, E.A. Craig, M.D. Fleming, Congenital sideroblastic anemia due to mutations in the mitochondrial HSP70 homologue HSPA9, *Blood*. 126 (2015) 2734–2738. doi:10.1182/blood-2015-09-659854.
- [20] S. Bekri, G. Kispal, H. Lange, E. Fitzsimons, J. Tolmie, R. Lill, D.F. Bishop, Human ABC7 transporter: gene structure and mutation causing X-linked sideroblastic anemia with ataxia with disruption of cytosolic iron-sulfur protein maturation, *Blood*. 96 (2000) 3256–3264.
- [21] Y. Bykhovskaya, K. Casas, E. Mengesha, A. Inbal, N. Fischel-Ghodsian, Missense mutation in pseudouridine synthase 1 (PUS1) causes mitochondrial myopathy and sideroblastic anemia (MLASA), *Am. J. Hum.*

- Genet. 74 (2004) 1303–1308. doi:10.1086/421530.
- [22] C.J. Ricketts, J.A. Minton, J. Samuel, I. Ariyawansa, J.K. Wales, I.F. Lo, T.G. Barrett, Thiamine-responsive megaloblastic anaemia syndrome: long-term follow-up and mutation analysis of seven families, *Acta Paediatr. Oslo Nor.* 1992. 95 (2006) 99–104. doi:10.1080/08035250500323715.
- [23] P.K. Chakraborty, K. Schmitz-Abe, E.K. Kennedy, H. Mamady, T. Naas, D. Durie, D.R. Campagna, A. Lau, A.K. Sendamarai, D.H. Wiseman, A. May, S. Jolles, P. Connor, C. Powell, M.M. Heeney, P.-J. Giardina, R.J. Klaassen, C. Kannengiesser, I. Thuret, A.A. Thompson, L. Marques, S. Hughes, D.K. Bonney, S.S. Bottomley, R.F. Wynn, R.M. Laxer, C.P. Minniti, J. Moppett, V. Bordon, M. Geraghty, P.B.M. Joyce, K. Markianos, A.D. Rudner, M. Holcik, M.D. Fleming, Mutations in TRNT1 cause congenital sideroblastic anemia with immunodeficiency, fevers, and developmental delay (SIFD), *Blood.* 124 (2014) 2867–2871. doi:10.1182/blood-2014-08-591370.
- [24] L.G. Riley, S. Cooper, P. Hickey, J. Rudinger-Thirion, M. McKenzie, A. Compton, S.C. Lim, D. Thorburn, M.T. Ryan, R. Giegé, M. Bahlo, J. Christodoulou, Mutation of the mitochondrial tyrosyl-tRNA synthetase gene, YARS2, causes myopathy, lactic acidosis, and sideroblastic anemia--MLASA syndrome, *Am. J. Hum. Genet.* 87 (2010) 52–59. doi:10.1016/j.ajhg.2010.06.001.
- [25] D.A. Lichtenstein, A.W. Crispin, A.K. Sendamarai, D.R. Campagna, K. Schmitz-Abe, C.M. Sousa, M.D. Kafina, P.J. Schmidt, C.M. Niemeyer, J. Porter, A. May, M.M. Patnaik, M.M. Heeney, A. Kimmelman, S.S. Bottomley, B.H. Paw, K. Markianos, M.D. Fleming, A recurring mutation in the respiratory complex 1 protein NDUF11 is responsible for a novel form of X-linked sideroblastic anemia, *Blood.* 128 (2016) 1913–1917. doi:10.1182/blood-2016-05-719062.
- [26] T. Matthes, P. Rustin, H. Trachsel, R. Darbellay, S. Costaridou, A. Xaidara, A. Rideau, P. Beris, Different pathophysiological mechanisms of intramitochondrial iron accumulation in acquired and congenital sideroblastic anemia caused by mitochondrial DNA deletion, *Eur. J. Haematol.* 77 (2006) 169–174. doi:10.1111/j.1600-0609.2006.00674.x.
- [27] S. Anderson, A.T. Bankier, B.G. Barrell, M.H. de Bruijn, A.R. Coulson, J. Drouin, I.C. Eperon, D.P. Nierlich, B.A. Roe, F. Sanger, P.H. Schreier, A.J. Smith, R. Staden, I.G. Young, Sequence and organization of the human mitochondrial genome, *Nature.* 290 (1981) 457–465.
- [28] D.C. Wallace, Mitochondrial genetics: a paradigm for aging and degenerative diseases?, *Science.* 256 (1992) 628–632.
- [29] A. Mansouri, B. Fromenty, A. Berson, M.A. Robin, S. Grimbirt, M. Beaugrand, S. Erlinger, D. Pessayre, Multiple hepatic mitochondrial DNA deletions suggest premature oxidative aging in alcoholic patients, *J. Hepatol.* 27 (1997) 96–102.
- [30] L.K. Kwong, R.S. Sohal, Age-related changes in activities of mitochondrial electron transport complexes in various tissues of the mouse, *Arch. Biochem. Biophys.* 373 (2000) 16–22. doi:10.1006/abbi.1999.1495.
- [31] M.-A. Robin, C. Demeilliers, A. Sutton, V. Paradis, C. Maisonneuve, S. Dubois, O. Poirel, P. Lettéron, D. Pessayre, B. Fromenty, Alcohol increases tumor necrosis factor alpha and decreases nuclear factor-kappaB to activate

- hepatic apoptosis in genetically obese mice, *Hepatology*. Baltim. Md. 42 (2005) 1280–1290. doi:10.1002/hep.20949.
- [32] A. Mansouri, I. Gaou, C. De Kerguenec, S. Amsellem, D. Haouzi, A. Berson, A. Moreau, G. Feldmann, P. Lettéron, D. Pessayre, B. Fromenty, An alcoholic binge causes massive degradation of hepatic mitochondrial DNA in mice, *Gastroenterology*. 117 (1999) 181–190.
- [33] J.R. Miller, R.W. Busby, S.W. Jordan, J. Cheek, T.F. Henshaw, G.W. Ashley, J.B. Broderick, J.E. Cronan, M.A. Marletta, Escherichia coli LipA is a lipoyl synthase: in vitro biosynthesis of lipoylated pyruvate dehydrogenase complex from octanoyl-acyl carrier protein, *Biochemistry (Mosc.)*. 39 (2000) 15166–15178.
- [34] A. Marquet, B.T. Bui, D. Florentin, Biosynthesis of biotin and lipoic acid, *Vitam. Horm.* 61 (2001) 51–101.
- [35] G. Liu, Y. Wang, G.J. Anderson, C. Camaschella, Y. Chang, G. Nie, Functional Analysis of GLRX5 Mutants Reveals Distinct Functionalities of GLRX5 Protein, *J. Cell. Biochem.* 117 (2016) 207–217. doi:10.1002/jcb.25267.
- [36] S. Bandyopadhyay, F. Gama, M.M. Molina-Navarro, J.M. Gualberto, R. Claxton, S.G. Naik, B.H. Huynh, E. Herrero, J.P. Jacquot, M.K. Johnson, N. Rouhier, Chloroplast monothiol glutaredoxins as scaffold proteins for the assembly and delivery of [2Fe-2S] clusters, *EMBO J.* 27 (2008) 1122–1133. doi:10.1038/emboj.2008.50.
- [37] S.L. Clarke, A. Vasanthakumar, S.A. Anderson, C. Pondarré, C.M. Koh, K.M. Deck, J.S. Pitula, C.J. Epstein, M.D. Fleming, R.S. Eisenstein, Iron-responsive degradation of iron-regulatory protein 1 does not require the Fe-S cluster, *EMBO J.* 25 (2006) 544–553. doi:10.1038/sj.emboj.7600954.
- [38] K. Furuyama, K. Kaneko, P.D. Vargas, Heme as a magnificent molecule with multiple missions: heme determines its own fate and governs cellular homeostasis, *Tohoku J. Exp. Med.* 213 (2007) 1–16.
- [39] P.R. Baker, M.W. Friederich, M.A. Swanson, T. Shaikh, K. Bhattacharya, G.H. Scharer, J. Aicher, G. Creadon-Swindell, E. Geiger, K.N. MacLean, W.-T. Lee, C. Deshpande, M.-L. Freckmann, L.-Y. Shih, M. Wasserstein, M.B. Rasmussen, A.M. Lund, P. Procopis, J.M. Cameron, B.H. Robinson, G.K. Brown, R.M. Brown, A.G. Compton, C.L. Dieckmann, R. Collard, C.R. Coughlin, E. Spector, M.F. Wempe, J.L.K. Van Hove, Variant non ketotic hyperglycinemia is caused by mutations in LIAS, BOLA3 and the novel gene GLRX5, *Brain J. Neurol.* 137 (2014) 366–379. doi:10.1093/brain/awt328.
- [40] P.B. Walter, M.D. Knutson, A. Paler-Martinez, S. Lee, Y. Xu, F.E. Viteri, B.N. Ames, Iron deficiency and iron excess damage mitochondria and mitochondrial DNA in rats, *Proc. Natl. Acad. Sci. U. S. A.* 99 (2002) 2264–2269. doi:10.1073/pnas.261708798.

Figures

Figure 1. Genetic studies in the cSA patient.

(A) Electropherograms of DNA extracted from the patient's peripheral blood leukocytes. Upon sequencing, p.Cys67Tyr and p.Met128Lys mutations were found in exons 1 and 2, respectively. The p.Cys67Tyr mutation was transmitted by the patient's father and the p.Met128Lys mutation by her mother..

(B) Protein sequences alignment showing that both mutated amino acids (Cys67 and Met128) are highly conserved across species.

(C) a. Ribbon representation of tetrameric GLRX5 3D structure (PDB 3WUL [17] in which are the amino acids Cys67 (C67) and Met128 (M128). The [2Fe-2S] cluster is shown in purple, the bound glutathione (GSH) in blue. b and c. Surface representation of the GLRX5 3D structure, focusing on Met128 and its neighborhood.

Figure 2. Impact of *GLRX5* mutations on heme biosynthesis.

CD34+ cells were isolated from the patient carrying the *GLRX5* mutations and healthy control as described in methods. The mRNA levels of ferrochelatase (Fech) (A) and ALAS2 (B) enzymes were measured by real-time PCR and their protein levels by western blotting (C) (blots on the left panel and quantification on the right panel). HPRT1 mRNA and tubulin protein were used as endogenous controls. The amount of intracellular PPIX was measured in CD34+ cells derived from *GLRX5* patient (D) and from EPP patients (E). The intracellular PPIX was also measured in *GLRX5* patient-derived CD34+ cells treated with ALA (ALA) or vehicle (NT). Bars represent minimum and maximum values with line at median.

Figure 3. Impact of *GLRX5* mutations on α -lipoic acid content.

α -lipoic acid (LA) content of KGDH (LA-KGDH) and PDH (LA-PDH) measured in triplicate (n=3) by western blot in LCL cells from the patient carrying the *GLRX5* mutations and healthy control (n=4) (blots on the left panel and LA ratio (on the right panel). GAPDH served as loading control. Bars represent minimum and maximum value with line at median.

Figure 4. Mitochondrial function in patient's LCL cells.

(A) Complexes I and IV activities, (B) Citrate synthase activity and (C) ATP level were measured in submitochondrial fractions isolated from LCL cells derived from the patient carrying the *GLXR5* mutations, patients with erythropoietic protoporphyria (EPP, n=5) and healthy control. Shown are mean \pm SD (n=3).

(D) Mitochondrial (mtDNA) and nuclear DNA (nDNA) content determined in LCL cells from the patient carrying the *GLXR5* mutations and healthy control (lower panel) by slot blot. Amplified 5942 and 464 pb mtDNA fragments are shown in the upper panel. (E) Circular, linear and supercoiled forms of mtDNA from LCL cells from the patient carrying the *GLXR5* mutations and healthy control assessed by southern blot.

(F) Cytochrome c oxidase, subunits 2 (COX2, upper panel) and 4 (COX4, lower panel) protein expression assessed by western blot in LCL cells derived from the patient carrying the *GLRX5* mutations and healthy control. Actin was used as loading control.

Figure 5. Impact of *GLRX5* mutations on iron metabolism in patient's LCL cells.

(A) Total ferritin level (ng/g of protein) was measured in total lysate from LCL cells derived from the patient carrying the *GLRX5* mutations and healthy control using a AU400 Automate. Shown are mean \pm SD (n=4).

(B) L-ferritin protein expression was determined by western blot in LCL cells derived from the patient carrying the *GLRX5* mutations and healthy control (blots on the left and quantification on the right). Actin served as loading control (n=4).

(C) TfR1 receptor level was measured by western blot (left panel) and flow cytometry (right panel) in LCL cells derived from the patient carrying the *GLRX5* mutations and healthy control. Actin served as loading control.

(D) IRP 1 (upper panel) and IRP 2 (lower panel) protein expression was measured by western blot in LCL cells derived from the patient carrying the *GLRX5* mutations and healthy control (blots on the left and quantification on the right). GAPDH was used as loading control.

(E) Mitochondrial, cytosolic and total aconitase activities were assessed in LCL cells derived from the patient carrying the *GLRX5* mutations and healthy control by measuring NADPH production (n=3).

Figure 6. Oxidative stress and cell proliferation in patient's LCL cells.

(A) Total GSH content (nmol/mg of protein) was measured and (B) MnSOD protein expression was determined by western blot in LCL cells derived from the patient carrying the *GLRX5* mutations and healthy control (n=4). (C) Cell proliferation was studied by MTT cell viability assay.

Tables

Table 1. Clinical and hematologic data from the parents (I.1; I.2), the siblings (II.1; II.2; II.4) and the patient carrying the *GLRX5* mutations (II. 3) at the time of diagnosis and at the 6-month and 1-year follow-up. RBC, red blood cells; Hb, hemoglobin; Hct, hematocrit; MCV, mean corpuscular volume; MCHC, mean corpuscular hemoglobin concentration; WBC, white blood cells; LDH, lactate dehydrogenase; LIC, liver iron content. Age and gender specific normal ranges are indicated in the right column.

Parameters	I.1	I.2	II.1	II.2	II.4	II.3 At diagnosis	II.3 6- month follow -up	II.3 1-year follow-up	Normal values
RBCs ($\times 10^{12}/L$)	5.12	4.45	4.85	4.56	5.22	5.28	4.36	5.18	4.1-5.1
Hb (g/dL)	14.1	13.5	14.5	14.2	15.1	8.9	6.4	9	11.5-16
Hct (%)	37	38	39	36	41	31.4	24,7	32.5	36-46
MCV (fL)	85	80	73	72	84	60	57	63	78-95
MCHC (g/dL)	34	33	29	31	33	28	26	28	30-36
WBC count ($\times 10^9/L$)	5.2	4.8	6.2	5.8	5.5	5	5.2	3.5	4.5-13.5
Reticulocytes (%)	ND	ND	ND	ND	ND	2.1	3.1	ND	

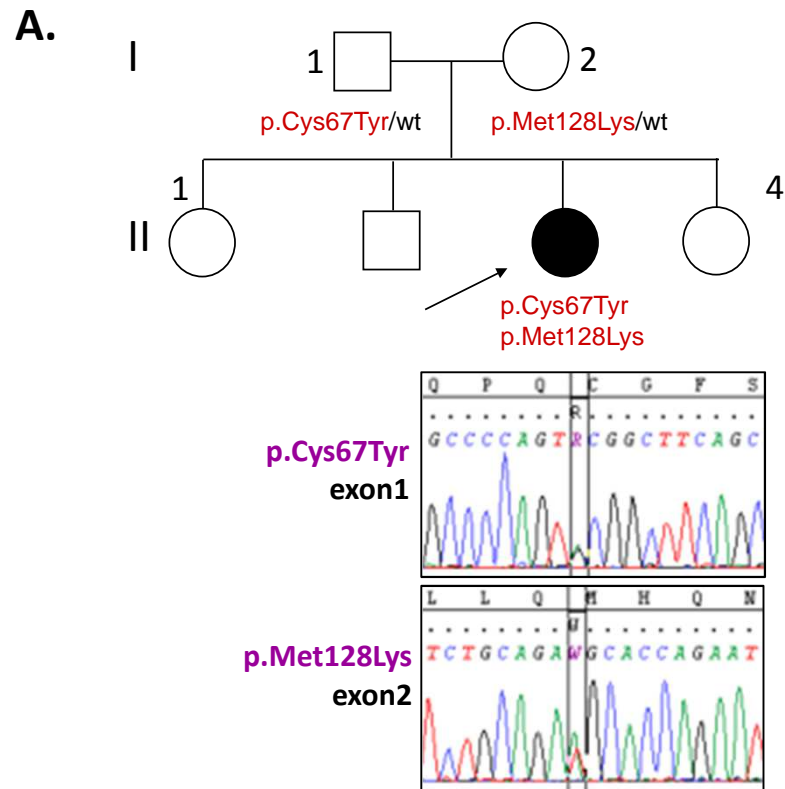
Bilirubin ($\mu\text{mol/L}$)	11	8	5	6	7	4.34	9	7	5-21
LDH (UI/L)	215	198	ND	ND	ND	385	ND	224	164-412
Iron ($\mu\text{mol/L}$)	ND	ND	ND	ND	ND	46.7	ND	34.9	12 –25
Transferrin (g/L)	ND	ND	ND	ND	ND	2.2	ND	3.9	2-3.8
Transferrin saturation	ND	ND	ND	ND	ND	85%	ND	36%	20-45%
Ferritin ($\mu\text{g/L}$)	311	180	85	75	102	466	191	71	12 – 300
Hepcidin (nmol/L)	ND	ND	ND	ND	ND	ND	ND	0.2	4-30
LIC ($\mu\text{mol/g}$)	ND	ND	ND	ND	ND	200	ND	ND	<36

Table 2. Porphyrins profile in erythrocytes, plasma and LCL cells from the patient carrying the *GLRX5* mutations and patients with erythropoietic protoporphyria (EPP).

Parameters	Patient	Normal Values ^a	EPP Patients (n=5)
Fech activity in LCL cells (nmol of zinc porphyrins/mg of protein/hr)	0.7	>3.5	1.2 ± 0.2
Porphyrins in erythrocytes			
Total porphyrins (µmol/L of RBC)	2.0	<1.9	24.9 ± 9.6
Zinc/free protoporphyrin ratio (%)	76	>72	11 ± 2.3
Porphyrins in plasma			
Total porphyrins (nmol/L)	<5	<20	281 ± 41

^a Normal value means the level of ferrochelatase activity in control LCL cultures and age and gender specific normal ranges. RBC: red blood cells.

Figure 1



B.

	67	128
<i>H. Sapiens</i>	GTPEQPQ C GFSNAV.....GCDILLQ M HQNGDLVE	
<i>M. mulatta</i>	GTPEQPQ C GFSNAV.....GCDILLQ M HQNGDLVE	
<i>O. Cuniculus</i>	GTPEQPQ C GFSNAV.....GCDILLQ M HQNGDLVE	
<i>R. Norvegicus</i>	GTPEQPQ C GFSNAV.....GCDILLQ M HQNGDLVE	
<i>M. Musculus</i>	GTPEQPQ C GFSNAV.....GCDILLQ M HQNGDLVE	
<i>D. Rerio</i>	GT P AQPM C GFSNAV.....GCDILLQ M HQSGDLVE	
<i>C. elegans</i>	GTQ Q EPAC C GFSRN V K.....GCDILIS M HKDGEISD	

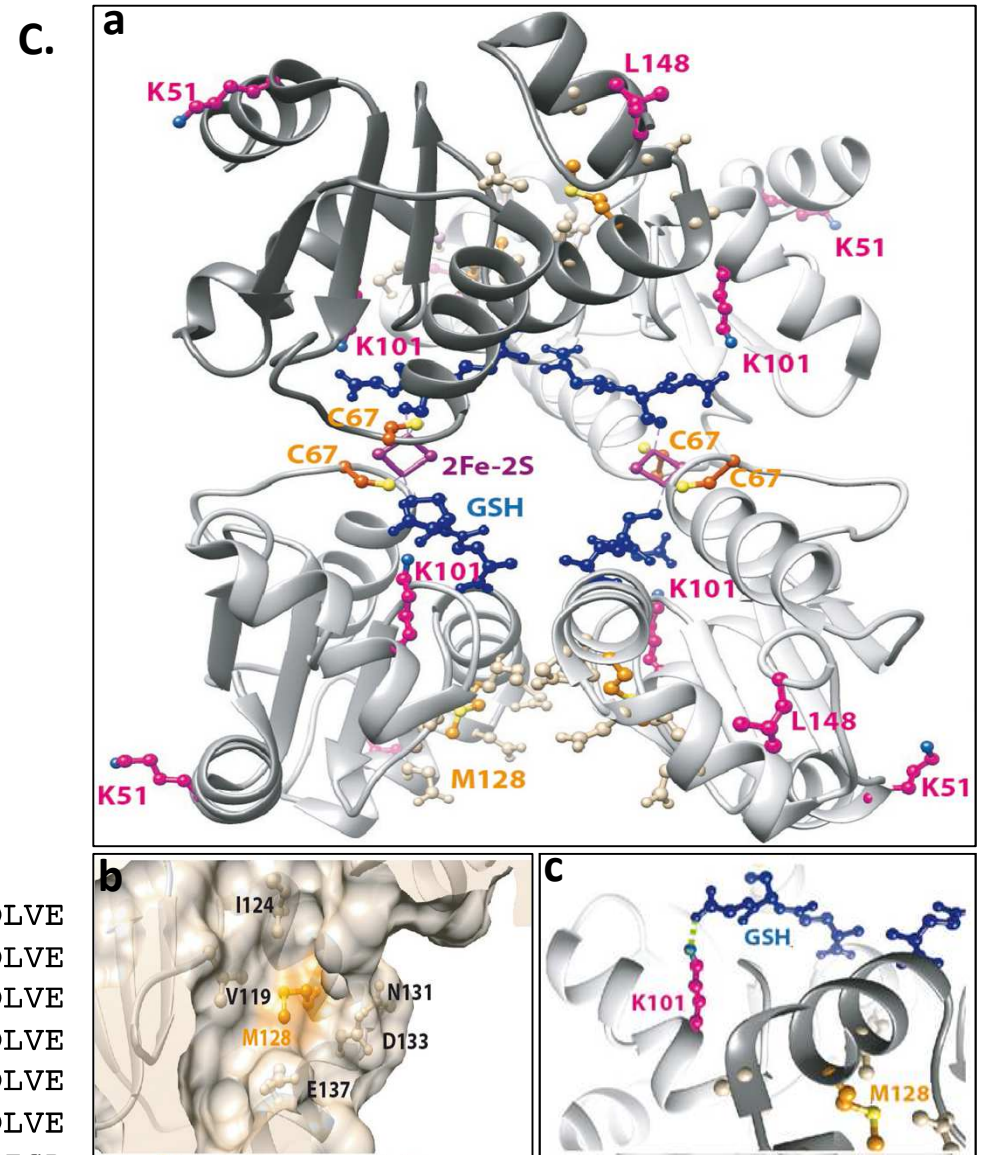


Figure 2

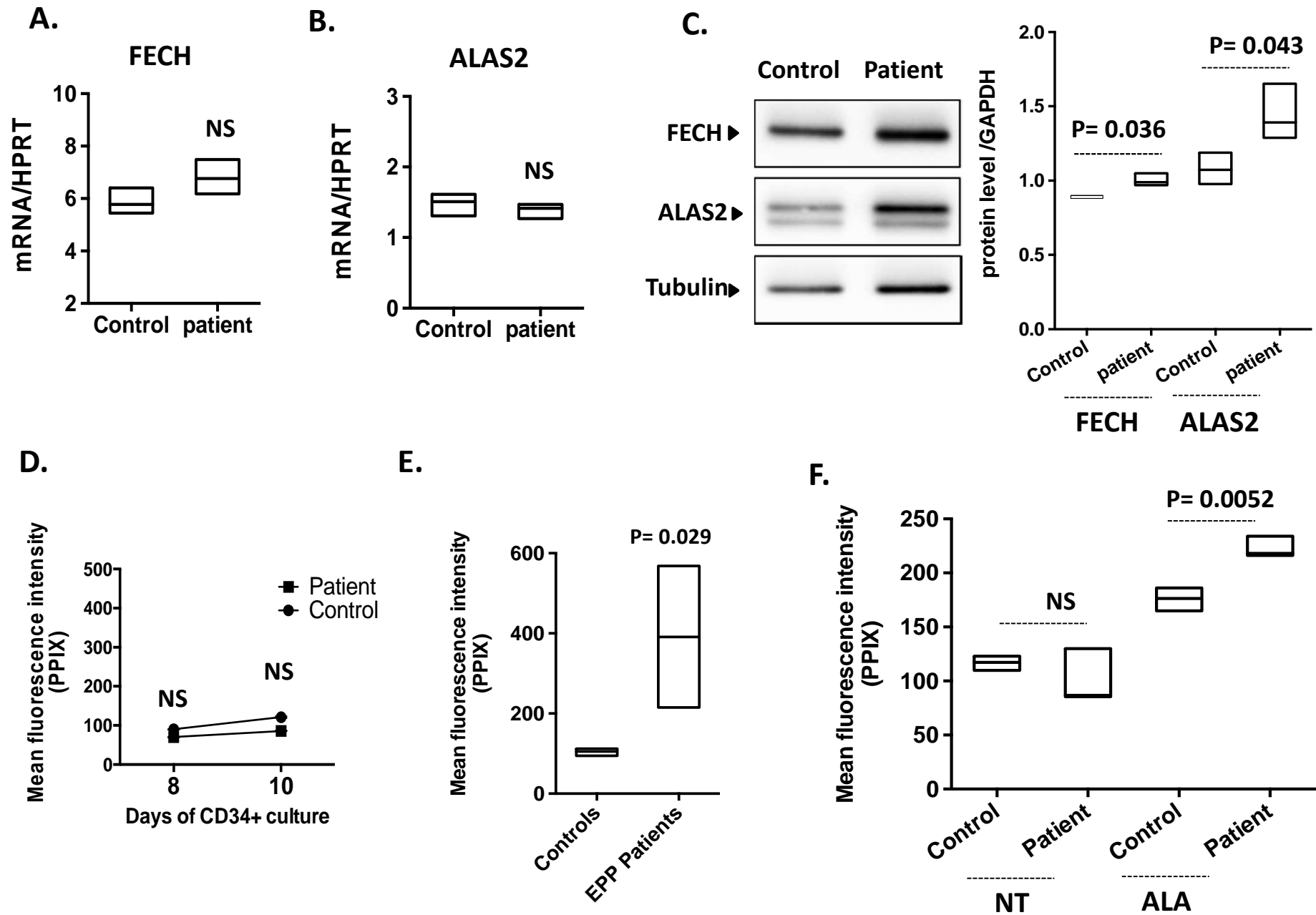
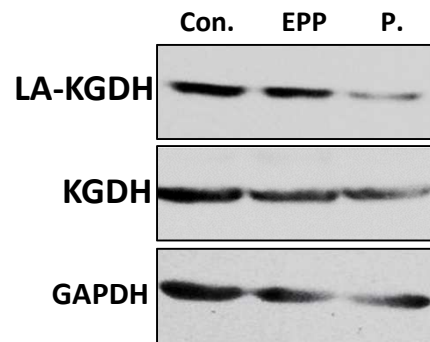
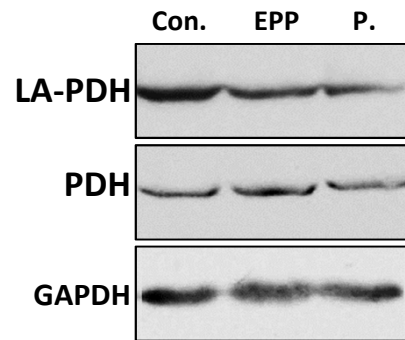


Figure 3

A.



B.



C.

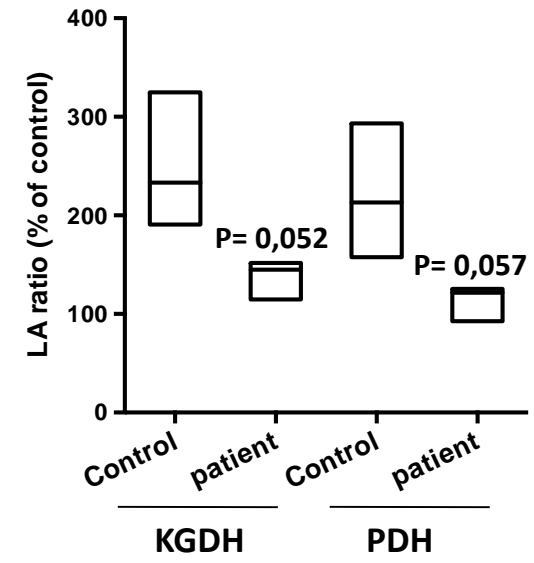


Figure 4

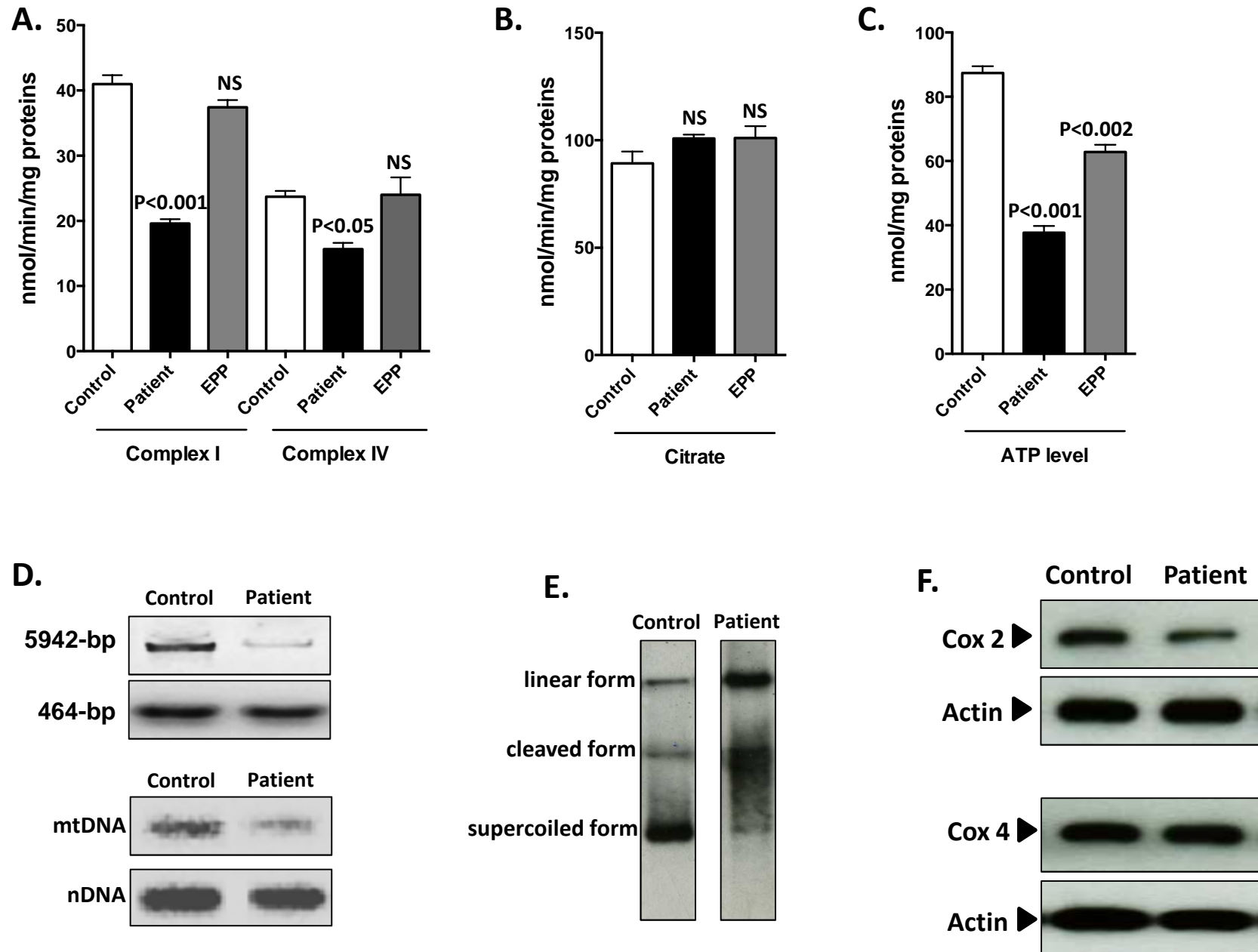


Figure 5

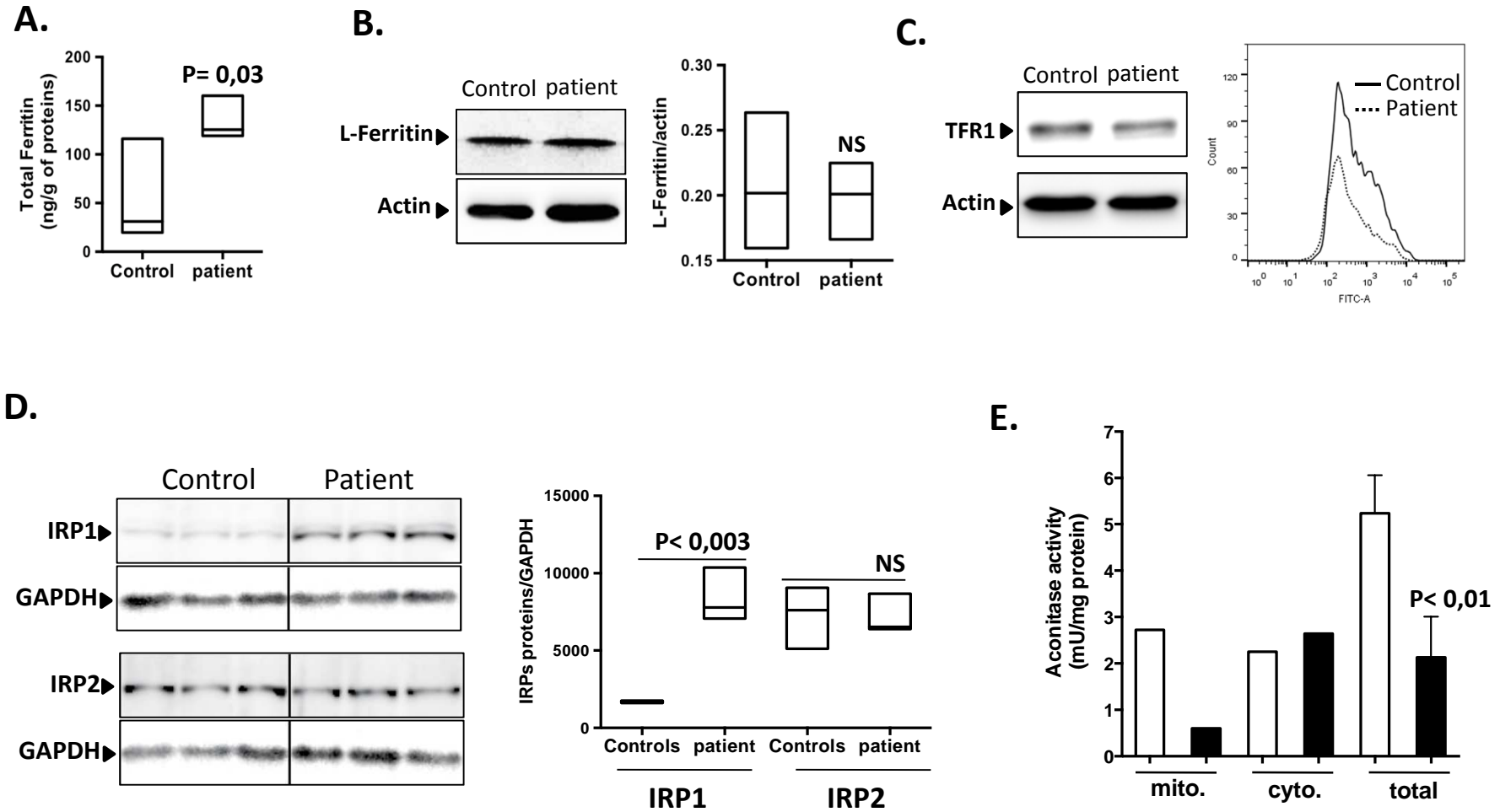


Figure 6:

